Neutrosophic Similarity Measure for Assessing Digital Watermarked Images

Taha Basheer Taha[1], Huda E. Khalid[2]*

[1] Telafer University, University Presidency, Research and Development Department, Telafer, Iraq;

E-mail: taha.b.taha@uotelafer.edu.iq

[2] Telafer University, The Administration Assistant for the President of the Telafer University,

Telafer, Iraq; https://orcid.org/0000-0002-0968-5611, dr.huda-ismael@uotelafer.edu.iq

* Correspondence: dr.huda-ismael@uotelafer.edu.iq

Abstract: Digital watermarking is an essential tool for numerous applications, and the quality of watermarked images must be assessed using accurate criteria. Peak Signal-to-Noise Ratio (PSNR), a widely used image assessment metric, has limits when evaluating images containing noise, such as watermarks. To tackle such kind of issues this, this study investigates a different assessment metric, the Neutrosophic Similarity Measure, and assesses its performance in evaluating watermarked images when compared to PSNR. Similarities to ascertain whether the neutrosophic similarity Measure has a higher noise tolerance and offers a more accurate evaluation of watermarked images. The results show that Neutrosophic Similarity Measure overcomes PSNR in capturing the influence of additive watermarks and demonstrating superior noise tolerance through experimental evaluation on a dataset of watermarked images. These findings highlight the possibility of adopting new assessment metric, such as neutrosophic similarity measure, for assessing watermarked images, thereby enhancing the effectiveness of evaluating watermarked Images.

Keywords: Digital Image Assessment; Watermark; Neutrosophic Similarity Measure, PSNR.

1. Introduction

Digital watermarking is a commonly used method for adding undetectable data—also referred to as watermarks—to digital assets including images, sounds, and video. In addition to copyright protection, these watermarks also verify data integrity and authenticate material. For determining the efficacy of watermarking algorithms and guaranteeing the preservation of imagine fidelity, the ability to reliably assess the quality of watermarked images is essential [1].

Peak Signal-to-Noise Ratio (PSNR) has been used extensively as a metric to assess the quality of watermarked images. By evaluating the ratio of peak signal strength to mean square error, PSNR evaluates the distinction between original and watermarked images. However, PSNR has certain limitations [2], it does not consider the perceptual impact of noise or distortion introduced by watermarks, and its effectiveness diminishes in scenarios involving additive noise.

To overcome these limitations, an alternative assessment metric which is neutrosophic similarity measure [3]has utilized in this paper. The utilization of neutrosophic similarity measure (NSM) as an assessment metric offers several advantages. It enables a more comprehensive analysis of watermarked image quality by considering the perceptual aspects, indeterminacy, and ambiguity. By capturing the impact of additive watermarks more effectively, neutrosophic similarity Measure can provide a better assessment of the overall fidelity and visual quality of watermarked images.

Considering the importance of digital watermarking and the limitations in its evaluation using traditional metrics like PSNR, exploring alternative assessment metrics such as neutrosophic similarity measure becomes imperative. This paper aims to compare the performance of PSNR and neutrosophic similarity Measure in evaluating watermarked images and ascertain the advantages of adopting a more robust assessment metric for accurate and reliable quality assessment.

2. Materials and Methods

2.1 Theoretical Background

In this section, a brief description of digital image processing and neutrosophic systems is presented.

2.1.1 Description of Digital Images

A digital image can be described as a two-dimensional function, $f(x, y)$, where x and y represent spatial coordinates, and the intensity or gray level of the image at any given (x, y) coordinate is determined by the value of f [4]. When both x, y, and the intensity values of f are discrete and finite, the image is referred to as a digital image. Digital image processing involves manipulating digital images using a computer. It's important to note that a digital image consists of a finite number of elements, each with a specific location and value. These elements are commonly referred to as picture elements, image elements, pels, or pixels. The term "pixel" is widely used to describe the elements of a digital image.

In the early days of the newspaper industry, digital images found one of their initial uses in transmitting pictures between London and New York via submarine cables. The introduction of the Bartlane cable picture transmission system during the early 1920s significantly decreased the time needed to transport a picture across the Atlantic Ocean, reducing it from over a week to under three hours. This system involved specific printing equipment that encoded pictures for transmission through the cables and reconstructed them upon reaching the receiving destination.

The image in Figure 1, created in 1921, was generated from a coded tape using a telegraph printer equipped with a unique typeface [5].

Figure 1. Telegrapher Printer Image in 1921

2.1.2 Digital Image Representation

A digital image serves as a numerical representation of a real image that can be stored and processed by a digital computer. The process begins by dividing the image into small areas known as pixels or picture elements. Each pixel corresponds to a specific location within the image and is associated with a numerical value or a set of numbers that describe certain properties of the pixel, such as its brightness or color. These numerical values are organized in an array format, with rows and columns representing the vertical and horizontal positions of the pixels in the image.

Digital images possess several fundamental characteristics. One important aspect is the image type, which can vary. For instance, a black and white image records only the intensity of light falling on the pixels. Color images, on the other hand, can consist of three colors (typically RGB - Red, Green, Blue) or four colors (CMYK - Cyan, Magenta, Yellow, black). RGB images are commonly used in computer monitors and scanners, while CMYK images are utilized in color printers. There are also non-optical images, like ultrasound or X-ray, where the intensity of sound or X-rays is recorded. In range images, the distance of each pixel from the observer is captured.

Resolution is another key characteristic of digital images and is measured in pixels per inch (PPI). Higher resolution results in a more detailed image. Computer monitors generally have a resolution of around 100 PPI, while printers have resolutions ranging from 300 PPI to over 1440 PPI. Consequently, images tend to appear better in print due to the higher resolution compared to a monitor [6]. The color depth, applicable to color images, refers to the number of bits used to represent the brightness or color information. More bits allow for a greater range of shades of gray or colors. For example, an RGB image with 8 bits per color has a total of 24 bits per pixel, commonly referred to as "true color." Each bit can represent two possible colors, resulting in a total of 16,777,216 possible colors. The grayscale image is represented by brightness using 8 bits value. The brightness of a pixel value of a grayscale image ranges from 0 (black) to 255 (white) [7]. Binary images typically have only one bit or two "colors," representing black and white (Figure 2).

The format of an image provides additional details on how the numerical values are arranged within the image file, including information about compression techniques employed, if any. Various formats are available, with popular ones including BMP (is a format native to the Windows operating system, JPEG (recognized for lossy compressing and encoding high-resolution digital images), PNG (images with lossless compression), and GIF (animated images) [8].
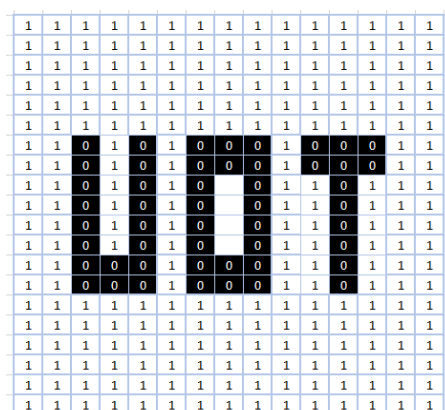

Figure 2. Binary Image

2.1.3 Digital Image Watermarking:

Image watermarking is the process of embedding a watermark signal (as a text or small binary image) into the cover image, which is the target that needs to be protected/tracked. Image watermarking can be considered as the basis for video watermarking as the video is a set of consecutive frames, where each frame can be considered as a separate image. A digital watermarking system consists of two main steps: embedding and extraction. In embedding, the watermark is embedded inside the host image, while in extraction, the watermark is retrieved from the host image. If the process of retrieving can be applied without the existing of the original image, then it is "blind Extraction", and if the host image is required for extraction, then it is non-blind extraction. Figures 3 shows the process of watermark embedding [1], [9]:

Generally, the watermarking process consists of the following major components.

- **Host** (Original) image: The target of the watermarking system that needs to be watermarked.
- **Watermark**: Information to be embedded, which might be the company logo, metadata, etc.
- **Key**: The encryption key that is used to encrypt the watermark before embedding to apply more security. The existence of the key is optional.
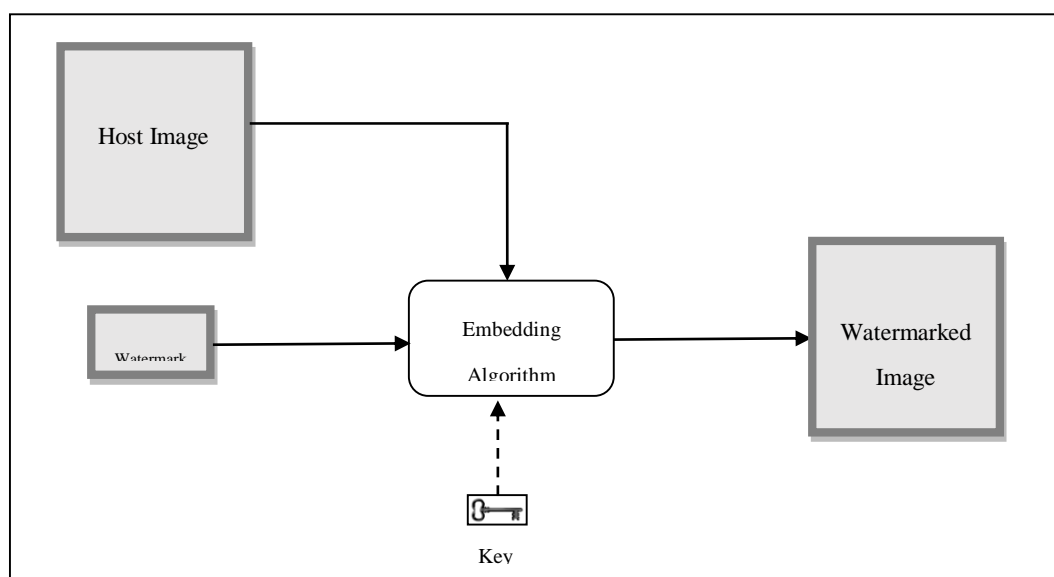- **Watermarked Image**: Image that implicitly contains the watermark.

Figure 3. Watermark Embedding Process

2.1.4 Neutrosophic Sets

Neutrosophic sets, introduced by Smarandache [3], provide a novel approach for addressing uncertainty by incorporating truth-membership (T), indeterminacy-membership (I), and falsity-membership (F) values within the range of $0 \leq T + I + F \leq 3$. Compared to intuitionistic fuzzy sets, these values provide a more thorough and precise description of ambiguous information. The idea of neutrosophic sets has received a lot of attention from researchers and has been expanded into a number of different fields. These extensions have found use in decision-making, information measures, image processing, graph theory, and algebraic structures. Neutrosophic sets rapidly became a tool for handling vagueness in a variety of real-life scenarios [10].

Numerous studies highlight the neutrosophic sets' quick development and adaptability, which enable quantitative and qualitative analyses from a variety of angles[11] [12]. The field of image processing has benefited greatly from the use of neutrosophic theory, particularly in the areas of edge detection and image segmentation. Neutrosophic offsets have been used to segment images successfully, offering a solid framework to deal with the ambiguity and uncertainty that come with image analysis. Neutrosophic offsets (when some neutrosophic components are off the interval [0, 1], i.e., some neutrosophic component > 1 and some neutrosophic component < 0 [10]) enable a thorough

characterization of image regions and boundaries by considering truth-membership, indeterminacy-membership, and falsity-membership values. Additionally, edge detection applications have been shown promise when using neutrosophic theory. The flexibility of these forms provides a method for capturing minute changes and transitions in edge information, improving the precision and dependability of edge detection algorithms [13].

Neurotrophic Similarity Measure: The neutrosophic similarity measure is a metric used within the neutrosophic framework to quantify the similarity between two neutrosophic sets or objects. Neutrosophic similarity measures consider the truth-membership, indeterminacy-membership, and falsity-membership values associated with the objects being compared. Similarity measure is calculated to identify the degree to the ideal object under intensity condition.

Neutrosophic similarity measure (NSM) calculation steps [14]**:**
1. Normalize the images to the range [0,1].
2. Calculate the positive, neutral, and negative memberships.
3. Calculate the numerator and denominator of the NSM.

$Numerator = sum \ (sum \ (min \ (a_1, a_2) + min \ (ap_1, ap_2) + min \ (an_1, an_2)))$ (1)

$Denominator = sum \ (sum \ (max \ (a_1, a_2) + max \ (ap_1, ap_2) + max \ (an_1, an_2)))$ (2)

Where a_1 is the host image, a_2 is the watermarked image; ap_1 is the positive membership of a_1, ap_2, is the negative membership of a_2. While an_1, an_2 are the negative membership of a_1 and a_2, respectively.

4. Calculate the NSM between the two images.

$NSM = Nominator \ / \ Denominator$ (3)

2.1.5 Image Quality Assessment:

For assessing the quality of digital images, there are two available methods. The initial method uses judgment from humans and is known as subjective assessment. Human observations, however, can differ greatly between people due to perception differences. To get a range of opinions, this calls for involving multiple subjects. However, it can be inconvenient, time-consuming, and expensive to conduct subjective experiments. Hence, it is not usually employed.

On the other hand, objective assessment offers an alternative strategy for computing-based image quality evaluation. In the literature, a variety of objective metrics have been placed out to evaluate the quality of images that have undergone compression, transformation, or other image processing operations. A single metric could not be able to adequately address all types of distortions, so it's important to note that different distortion types may call for the use of multiple metrics[15].

For watermarked images, Peak signal to noise ratio ($PSNR$) is a common metric that is used in literature studies for watermarked image assessment [16][17], and its equation is based on calculating the mean square error as shown in the following equations:

$$PSNR = 20 \ \log_{10}\left(\frac{255}{\sqrt{MSE}}\right)$$ (4)

And

$$MSE = \frac{1}{m \times n} + \sum_{i=1}^{m} \sum_{j=1}^{n} \| \ X(i,j) - \ Y\ (i,j) \ \|^{\ 2} \tag{5}$$

Where X and Y represent the original and altered images, respectively, with dimensions m and n. The indices i and j are used to denote individual pixels within the images.

However, the bias of Human Vision System (HVS) in observing the noise in different image structures is not considered by $PSNR$ [18] .

Hence, in this paper, neutrosophic similarity measure (NSM) will be utilized to assess the quality of watermarked images and to be compared with $PSNR$.

2.2 Literature Studies

Numerous studies and comparisons of various measures for assessing the quality of watermarked images have been conducted in literature. A comprehensive review of a number of quality metrics was carried out in study [15] to determine the best metric for assessing watermarked images. The performance of the metrics in evaluating the quality of watermarked images was examined and contrasted. The metrics "PSNR_wav2" and "Komparator" were discovered to be most relevant and useful for assessing the overall quality of watermarked images out of the many that were evaluated. In another notable research by Kutter et.al [19] focus was on addressing the challenges associated with fair benchmarking and the evaluation of digital watermarking methods. This study not only aimed to identify suitable evaluation metrics but also proposed a novel metric specifically designed for the evaluation of watermarked images. The proposed metric aimed to provide a more comprehensive and accurate assessment of the visual quality of watermarked images, considering factors such as robustness, perceptual transparency, and resistance to attacks.

Additionally, in another experiment [20], in which an image quality metric based on singular value decomposition (SVD) was used to improve the evaluation of watermarked image visual quality. Several watermarking methods' performance was evaluated using the SVD-based metric. In order to evaluate the visual quality of watermarked images, fidelity, distortion, and robustness against typical image processing operations were taken into account.

These literature examples highlight the ongoing research efforts to improve the evaluation of watermarked images through the exploration, comparison, and refinement of various evaluation metrics. By identifying and utilizing suitable metrics, researchers aim to enhance the accuracy, reliability, and effectiveness of evaluating the quality and performance of watermarked images in different applications and scenarios.

E. F-Navarro et al. [21] proposed a set of assessment metrics for visible watermarking algorithms. These metrics consist of four components: visibility assessment, global obtrusiveness assessment, local obtrusiveness assessment, and global quality assessment. They are based on the characteristics of the Human Visual System (HVS) and utilize the concept of Just Noticeable Difference (JND) functions (JND is the maximum sensory distortion that human eye does not percieve [22]) . The mentioned metrics require the input of the host image, watermark pattern, and visible watermarked image for evaluation, and the existing of watermarking pattern and the original watermark may not be possible in all cases. These image evalaution metrics were found to be particularly useful in

evaluating the robustness of watermark removal and assessing the visibility and quality of attacked watermarked images.

To the best of our knowledge, the utilization of the neutrosophic framework with its ambiguity and uncertainty in the creation of a metric for digital image evaluation, specifically for watermarked images, has not been explored in literature and its usage may lead to promising results for evaluating watermarked images and it also can participate in developing watermarking algorithms.

2.3 Proposed Work

The methodology employed in this paper involves two main stages: watermark embedding and the assessment of the watermarked images. In the first stage, the binary watermark, as illustrated in Figure 4, was incorporated into ten standard images of size 512×512 pixels. Host image thumbnails, shown in Figure 5, provide a visual representation of the chosen images. To ensure consistency across different image sizes, the watermark was embedded four times in each host image. The binary watermark consists of pixels with binary values of either zero or one, representing the black and white colors, respectively. To prevent issues arising from multiplication by zero during the embedding process, each zero value in the watermark was transformed to -1, which was then multiplied by the embedding power (ep). The selection of the ep value directly influences the watermark's strength, enabling the analysis of various distortion levels. By varying the ep value, a range of distortion scenarios can be examined, providing valuable insights into the watermark's robustness under different conditions.

Figure 4: Binary Watermark

Figure 5: Tested Host Images (Numbered as I1-I10, starting from top left)

The watermark was embedded into the images at five different intensities: $2, 4, 6, 8,$ and 10. This range of embedding intensities allowed for a comprehensive assessment of the watermark's performance under varying degrees of strength. For each embedded image, two evaluation metrics were used: the Peak Signal-to-Noise Ratio (*PSNR*) and the Neutrosophic Similarity Measure (*NSM*). The *PSNR*, a commonly used objective metric, quantifies the quality of the watermarked image by measuring the ratio of the peak signal power to the distortion caused by the watermark embedding

process. Higher *PSNR* values indicate better preservation of image quality, with less distortion introduced by the watermark.

NSM was employed as a new metric specifically designed for assessing the quality and similarity of watermarked images within the neutrosophic framework. The *NSM* takes into account the truth-membership, indeterminacy-membership, and falsity-membership values. Figure 6 shows the process of watermarked image evaluation.
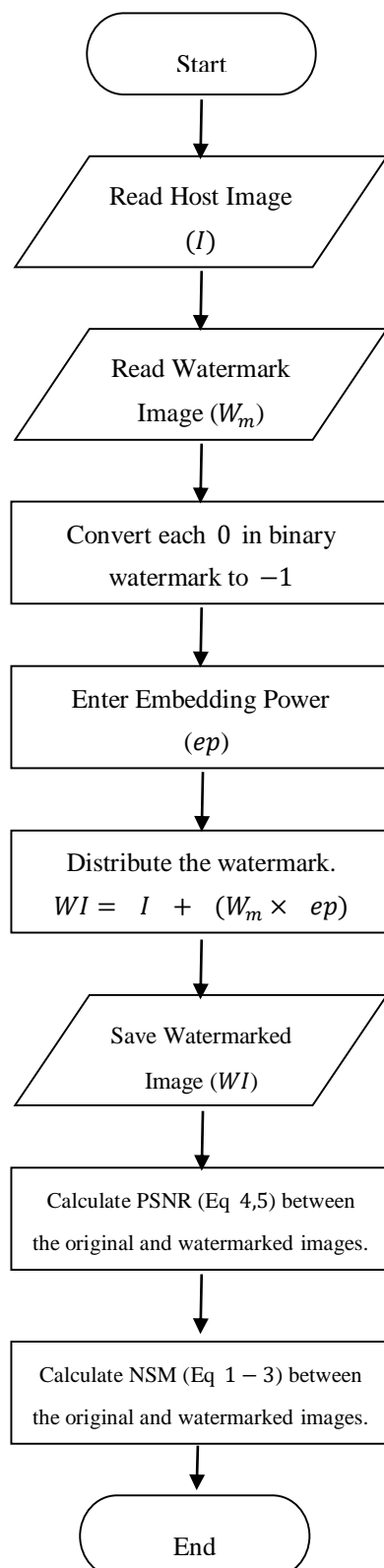
```
          ┌─────────────┐
          │    Start     │
          └──────┬──────┘
                 │
        ╱──────────────────╲
       ╱  Read Host Image    ╲
       ╲        (I)          ╱
        ╲──────────────────╱
                 │
        ╱──────────────────╲
       ╱  Read Watermark     ╲
       ╲  Image (Wₘ)         ╱
        ╲──────────────────╱
                 │
       ┌────────────────────┐
       │ Convert each 0 in   │
       │ binary watermark    │
       │ to −1               │
       └─────────┬──────────┘
                 │
       ┌────────────────────┐
       │ Enter Embedding     │
       │ Power (ep)          │
       └─────────┬──────────┘
                 │
       ┌────────────────────┐
       │ Distribute the      │
       │ watermark.          │
       │ WI = I + (Wₘ × ep)  │
       └─────────┬──────────┘
                 │
        ╱──────────────────╲
       ╱  Save Watermarked   ╲
       ╲  Image (WI)         ╱
        ╲──────────────────╱
                 │
       ┌────────────────────┐
       │ Calculate PSNR      │
       │ (Eq 4,5) between    │
       │ the original and    │
       │ watermarked images. │
       └─────────┬──────────┘
                 │
       ┌────────────────────┐
       │ Calculate NSM       │
       │ (Eq 1 − 3) between  │
       │ the original and    │
       │ watermarked images. │
       └─────────┬──────────┘
                 │
          ┌─────────────┐
          │     End      │
          └─────────────┘
```

The flowchart describes the process of watermarked image evaluation. It begins with **Start**, then **Read Host Image (I)**, **Read Watermark Image (W_m)**, **Convert each 0 in binary watermark to -1**, **Enter Embedding Power (ep)**, **Distribute the watermark. $WI = I + (W_m \times ep)$**, **Save Watermarked Image (WI)**, **Calculate PSNR (Eq 4,5) between the original and watermarked images.**, **Calculate NSM (Eq $1-3$) between the original and watermarked images.**, and **End**.

Figure 6: Process of Watermarked Image Evaluation

3. Results

In this section the results of embedding will be depicted, in addition to the results of *PSNR* and *NSM* metrics. A comparison between the two metrics is presented at the end of the section.

3.1. Watermark Embedding Results

Watermark had been embedded four times in each host image. Figure 7 shows the results after embedding in different intensities.
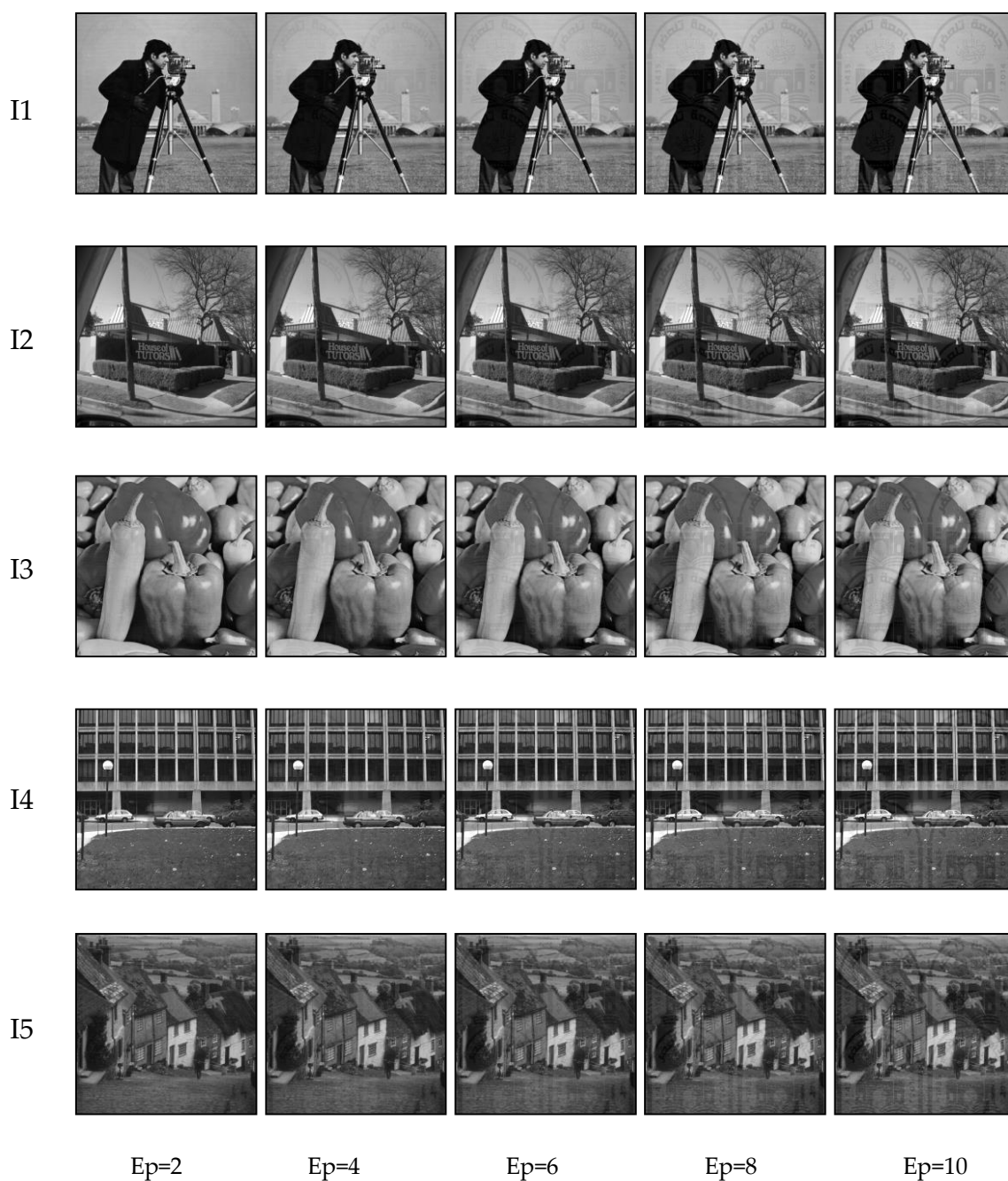

| | Ep=2 | Ep=4 | Ep=6 | Ep=8 | Ep=10 |

Figure 7: Watermarked Images with Different Embedding Intensities (**Cont**.)
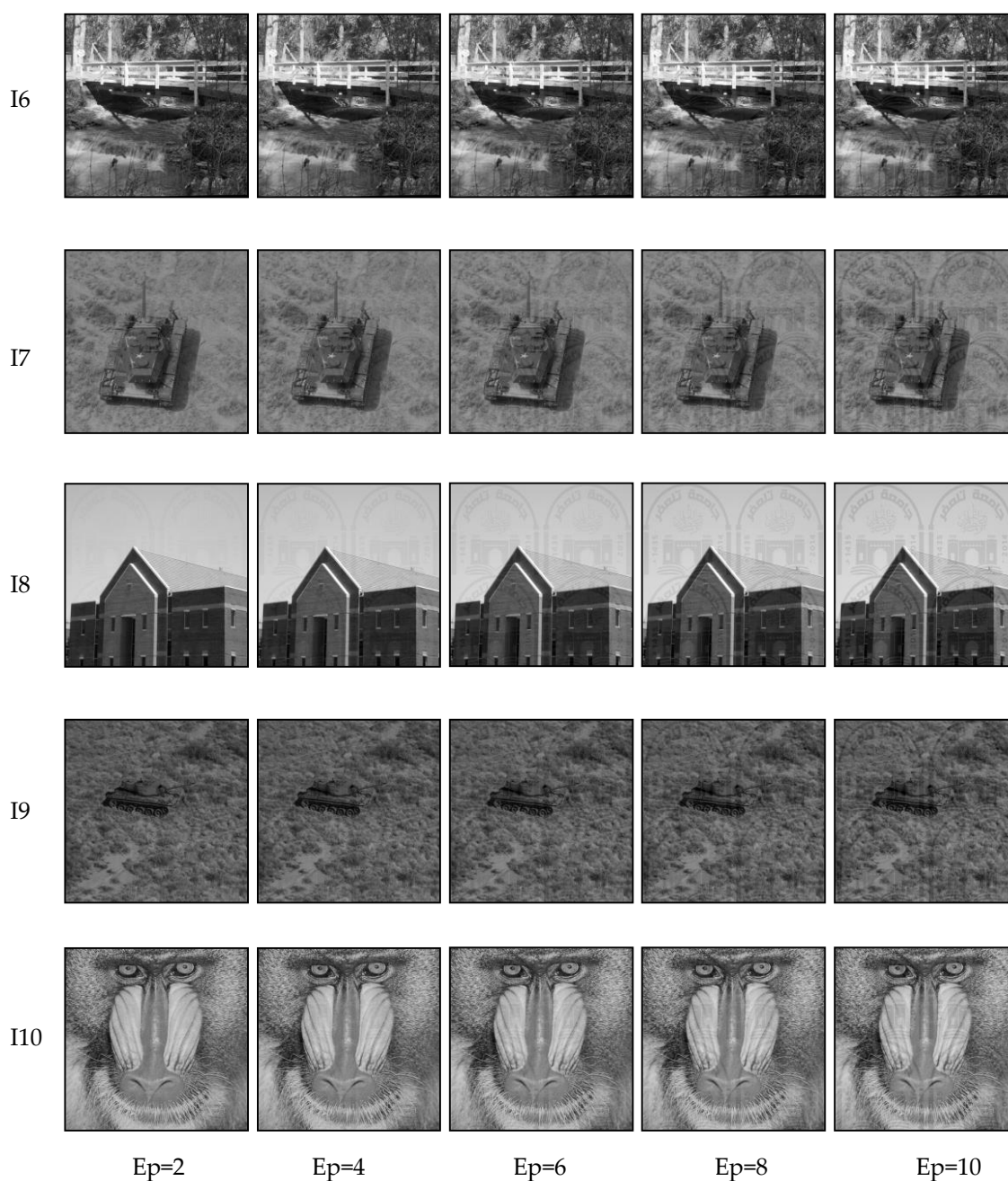
Figure 7: Watermarked Images with Different Embedding Intensities

Figure 7 makes clear that even at the same embedding intensities, the perceptibility of the watermark varies between the tested images. In Image I8, which has a lot of large smooth areas like the sky, it is important to note that even with an embedding intensity of 2, the watermark is still visible. In contrast, the watermark is less noticeable at intensities 4 and 6 in images with more complex content, such $I7$ and $I10$. This variation in watermark visibility can be related to the images' various characteristics and texture amount and distribution. Extensive smooth areas might make a watermark more noticeable, whereas complex textures and details can partially hide its appearance. These observations highlight the importance of considering image content and structure when assessing the perceptibility of watermarks at different intensities. However, there are other

factors are involved in visual quality, as high intensities and low intensities, and the textures are appeared more visible to human eye when it positioned in the edges [16].

3.2. *PSNR* and *NSM* Values:

Tables $1-5$ present the results of the evaluation conducted on the tested images, providing the values of both Peak Signal-to-Noise Ratio (*PSNR*) and Neutrosophic Similarity Measure (*NSM*) for various embedding intensities. Each table corresponds to a specific embedding intensity, namely $2, 4, 6, 8,$ and $10.$ The *PSNR* values indicate the level of signal degradation caused by the watermark embedding process, with higher values indicating better image quality. On the other hand, the *NSM* values reflect the similarity between the watermarked images and their corresponding original counterparts, with higher values indicating a stronger resemblance. By examining these tables, it is possible to analyze the impact of different embedding intensities on both the signal quality and the similarity measure, providing valuable insights into the performance of the watermarking algorithm under different settings

Table 1. PSNR and NSM Values for Ep=2

Image	PSNR	NSM
I1	42.1129	0.98704
I2	42.1126	0.98706
I3	42.1102	0.98713
I4	42.1342	0.98692
I5	42.1102	0.98705
I6	42.1271	0.98695
I7	42.1102	**0.98789**
I8	42.1193	**0.9866**
I9	42.1102	0.98731
I10	42.1109	**0.98749**

Table 2. PSNR and NSM Values for Ep=4

Image	PSNR	NSM
I1	36.0934	0.97429
I2	36.0968	0.97436
I3	36.0899	0.97446
I4	36.1181	0.97405
I5	36.0896	0.9743
I6	36.1065	0.97413
I7	36.0896	**0.97621**
I8	36.1000	0.97339
I9	36.0896	**0.97484**
I10	36.0906	**0.97521**

Table 3. PSNR and NSM Values for Ep=6

Image	PSNR	NSM
I1	32.5731	0.96174
I2	32.5778	0.96189
I3	32.5687	0.96199
I4	32.5989	0.96139
I5	32.5678	0.96177
I6	32.5856	0.96152
I7	32.5678	**0.96486**
I8	32.5794	0.96037
I9	32.5678	**0.96257**
I10	32.5691	**0.96317**

Table 4. PSNR and NSM Values for Ep=8

Image	PSNR	NSM
I1	30.0770	0.9494
I2	30.0807	0.94961
I3	30.0716	0.94972
I4	30.1018	0.94893
I5	30.0690	0.94943
I6	30.0880	0.94909
I7	30.0690	**0.9538**
I8	30.0822	0.94753
I9	30.0690	**0.9505**
I10	30.0706	**0.95134**

Table 5. PSNR and NSM Values for Ep=10

Image	PSNR	NSM
I1	28.1530	0.93733
I2	28.1438	0.93754
I3	28.1373	0.93765
I4	28.1652	0.93666
I5	28.1308	0.93729
I6	28.1510	0.93687
I7	28.1308	**0.94295**
I8	28.1465	**0.93487**
I9	28.1314	0.93864
I10	28.1326	**0.93972**

The analysis of the obtained results from Tables $1-5$ reveals several key observations. Firstly, the $PSNR$ values exhibit variations ranging from $42dB$ to $28dB$ across the different embedding power levels of 2 to 10. It is worth noting that the $PSNR$ values remain relatively consistent among all the tested images, suggesting a consistent level of signal degradation caused by the watermark embedding process. On the other hand, the NSM values exhibit a better behavior. Despite minor variations and a relatively limited range between 0.98 and 0.93, the NSM values demonstrate higher perceptual quality in all embedding intensities for images with higher texture, such as $I7, I9$, and $I10$. Conversely, images like $I8$, characterized by smoother features and lower texture, consistently yield lower NSM values compared to the other images.

The values of NSM are normalized between $0-1$, while $PSNR$ values are results of logarithmic equations where changes can have more impact on the obtained results. Hence, the changes in embedding intensity have higher impact in $PSNR$ than NSM.

However, the NSM values require scaling to accurately reflect the observed changes, they can serve as a valuable assessment measurement for evaluating the quality of watermarked images. These findings suggest that the NSM metric is sensitive to the perceptual characteristics of the images and can provide insights into the effectiveness of the watermarking algorithm in preserving image quality and similarity to the original content.

Figure 8 shows the variation of changes in low textured image $I1$ and High textured image $I7$ for $PSNR$. And NSM for the same images is shown in Figure 9. Similar results will be obtained by using $I8$ with $I10$.
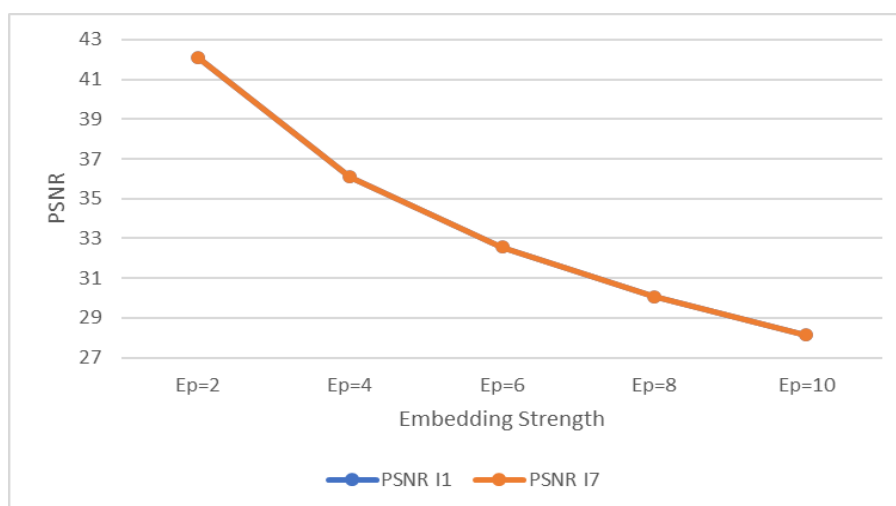
Figure 8: *PSNR* values for low textured image *I*1 and high Textured Image *I*7
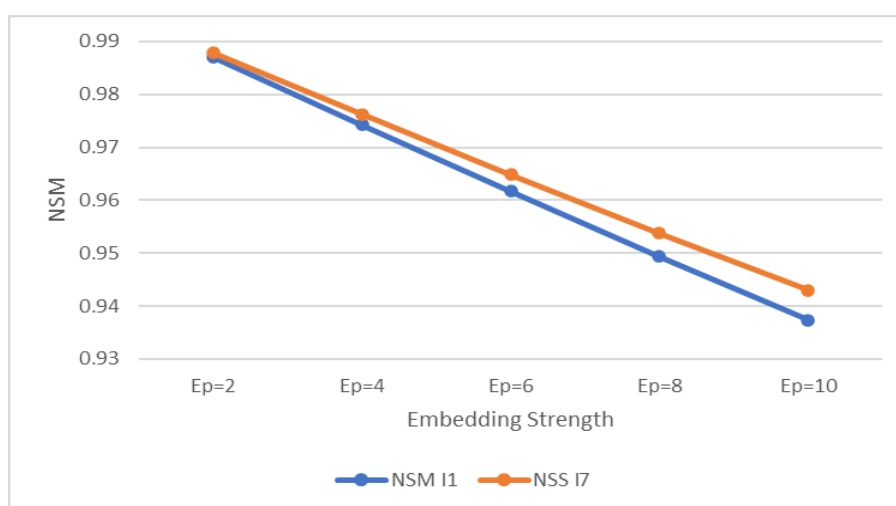

Figure 9: NSM values for low textured image *I*1 and high Textured Image *I*7

The comparative analysis between the *PSNR* and *NSM* metrics reveals notable distinctions in their performance. It is observed that the *PSNR* curves for both images are nearly identical, with one curve being consistently displayed above the other on the graph. This implies that the *PSNR* metric assigns similar values to both images, irrespective of the texture or structure of the image. In contrast, the *NSM* metric demonstrates a different behavior, where an increase in the amount of noise (embedding strength) leads to greater dissimilarity between the two images. Notably, the *NSM* metric exhibits a preference for high-textured images, as they are less affected by noise and consequently yield higher *NSM* values. This highlights the superiority of the *NSM* metric over *PSNR* in simulating the sensitivity of the Human Visual System (*HVS*) to noise. By capturing the perceptual aspects and incorporating image texture information, the *NSM* metric offers a more comprehensive and accurate evaluation of image quality, surpassing the limitations of *PSNR*.

4. Applications

These are some applications that highlight the practical implications of the study's findings in image processing field:

- Image Quality Assessment: The *NSM* metric can be utilized as a perceptual quality assessment tool for image processing algorithms, including watermarking techniques.

It can help determine the effectiveness of different watermark embedding strengths in preserving image quality.

- Watermarking Algorithm Optimization: By analyzing the performance of different embedding intensities and their corresponding *NSM* values, this study can aid in optimizing watermarking algorithms to achieve the best balance between robustness and perceptual quality.
- Creating a new Just Noticeable Distortion (*JND*) model to simulate human vision system in perceiving noise.
- Image Authentication and Forensics: The comparative analysis between *PSNR* and NSM metrics provides insights into the sensitivity of watermarking algorithms to noise and image texture. This information can be applied to image authentication and forensic investigations to assess the integrity and authenticity of watermarked images.
- Content Protection and Copyright Verification: Watermarking is often used for copyright protection and content verification purposes. The findings of this study can contribute to the selection of appropriate watermark embedding strengths, ensuring optimal protection of intellectual property while maintaining acceptable visual quality.
- NSM can be combined with other image evaluation metrics as structural Similarity Index (*SSIM*) [23] to achieve better evaluation results.

5. Conclusion

This study has explored the limitations of the widely used Peak Signal-to-Noise Ratio (*PSNR*) metric in evaluating watermarked images and has introduced the Neutrosophic Similarity Measure (*NSM*) as an alternative assessment metric. The experimental evaluation conducted on a dataset of watermarked images has demonstrated that *NSM* surpasses *PSNR* in capturing the influence of additive watermarks and exhibits superior noise tolerance. This was achieved because *NSM* values exhibited a better behavior, with minor variations and higher perceptual quality for images with higher texture. the study's findings underscore the importance of utilizing accurate assessment criteria for watermarked images, and the Neutrosophic Similarity Measure has demonstrated its potential to address the limitations of traditional metrics like *PSNR*, thereby advancing the field of digital watermarking. Future research can enhance watermarking algorithms by further exploring the impact of utilizing the *NSM* to find the best watermark embedding intensities.

Conflicts of Interest: The authors declare no conflict of interest.

References

[1] I. J. Cox, M. L. Miller, J. A. Bloom, J. Fridrich, T. Kalker, and J. Fridrich, *Digital Watermarking and Steganography*. Morgan Kaufmann, 2008.

[2] Z. Kotevski and P. Mitrevski, "Experimental Comparison of PSNR and SSIM Metrics for Video Quality Estimation," in *ICT Innovations 2009*, Berlin, Heidelberg: Springer Berlin Heidelberg, 2010, pp. 357–366. doi: 10.1007/978-3-642-10781-8_37.

[3] Smarandache F, *Neutrosophic Probability, Set, And Logic (first version)*. 2000. doi: 10.5281/zenodo.57726.

[4] Q. Gao and F.-F. Yin, "Two-Dimensional Direction-Based Interpolation with Local Centered Moments," 1999. [Online]. Available: http://www.idealibrary.comon

[5] R. C. Gonzalez and R. E. (Richard E. Woods, *Digital image processing*. 2018.

[6] Gregory A. Baxes, "Digital Image Processing: Principles and Applications," *Wiley*, Sep. 1994.

[7] C. Saravanan, "Color image to grayscale image conversion," in *2010 2nd International Conference on Computer Engineering and Applications, ICCEA 2010*, 2010, pp. 196–199. doi: 10.1109/ICCEA.2010.192.

[8] J. Miano, *Compressed image file formats: JPEG, PNG, GIF, XBM, BMP*. Addison Wesley, 1999.

[9] F. Hartung and M. Kutter, "Multimedia watermarking techniques," *Proceedings of the IEEE*, vol. 87, no. 7, pp. 1079–1107, Jul. 1999, doi: 10.1109/5.771066.

[10] F. Smarandache, H. E. Khalid, and A. K. Essa, "Neutrosophic Logic: The Revolutionary Logic in Science and Philosophy -- Proceedings of the National Symposium," 2018. [Online]. Available: https://digitalrepository.unm.edu/math_fsphttps://digitalrepository.unm.edu/math_fsp/205

[11] H. E. Khalid, "Neutrosophic Sets and Systems Neutrosophic Sets and Systems Neutrosophic Geometric Programming (NGP) with (max-product) Neutrosophic Geometric Programming (NGP) with (max-product) Operator, An Innovative Model Operator, An Innovative Model." [Online]. Available: https://digitalrepository.unm.edu/nss_journal

[12] X. Peng and J. Dai, "A bibliometric analysis of neutrosophic set: two decades review from 1998 to 2017," *Artif Intell Rev*, vol. 53, no. 1, pp. 199–255, Jan. 2020, doi: 10.1007/s10462-018-9652-0.

[13] F. Smarandache, M. A. Quiroz-Martínez, J. Estupiñan Ricardo, N. Batista Hernández, and M. Y. Leyva Vázquez, "APPLICATION OF NEUTROSOPHIC OFFSETS FOR DIGITAL IMAGE PROCESSING," 2020.

[14] S. Broumi and F. Smarandache, "Several Similarity Measures of Neutrosophic Sets," *Neutrosophic Sets and Systems*, vol. 1, 2013.

[15] P. B. Nguyen, M. Luong, and A. Beghdadi, "Statistical Analysis of Image Quality Metrics for Watermark Transparency Assessment," 2010, pp. 685–696. doi: 10.1007/978-3-642-15702-8_63.

[16] M. Barni, F. Bartolini, and A. Piva, "Improved wavelet-based watermarking through pixel-wise masking," *IEEE Transactions on Image Processing*, vol. 10, no. 5, pp. 783–791, 2001, doi: 10.1109/83.918570.

[17] X. Ma and X. Shen, "A novel blind grayscale watermark algorithm based on SVD," *ICALIP 2008 - 2008 International Conference on Audio, Language and Image Processing, Proceedings*, pp. 1063–1068, 2008, doi: 10.1109/ICALIP.2008.4590092.

[18] T. B. Taha, R. Ngadiran, and P. Ehkan, "Adaptive Image Watermarking Algorithm Based on an Efficient Perceptual Mapping Model," *IEEE Access*, vol. 6, pp. 66254–66267, 2018, doi: 10.1109/ACCESS.2018.2878456.

[19] F. A. P. Petitcolas, "Fair evaluation methods for image watermarking systems," *J Electron Imaging*, vol. 9, no. 4, p. 445, Oct. 2000, doi: 10.1117/1.1287594.

[20] A. Shnayderman and A. M. Eskicioglu, "Evaluating the visual quality of watermarked images," E. J. Delp III and P. W. Wong, Eds., Feb. 2006, p. 607222. doi: 10.1117/12.641972.

[21] E. Fragoso-Navarro, M. Cedillo-Hernandez, M. Nakano-Miyatake, A. Cedillo-Hernandez, and H. M. Perez-Meana, "Visible watermarking assessment metrics based on just noticeable distortion," *IEEE Access*, vol. 6, pp. 75767–75788, 2018, doi: 10.1109/ACCESS.2018.2883322.

[22]   A. Liu, W. Lin, M. Paul, C. Deng, and F. Zhang, "Just noticeable difference for images with decomposition model for separating edge and textured regions," *IEEE Transactions on Circuits and Systems for Video Technology*, vol. 20, no. 11, pp. 1648–1652, 2010, doi: 10.1109/TCSVT.2010.2087432.

[23]   Z. Wang, A. C. Bovik, R. H. Sheikh, and P. E. Simoncelli, "Wavelets for Image Image quality assessment: From error visibility to structural similarity," *IEEE Transactions on Image Processing*, vol. 13, no. 4, pp. 600–612, 2004, doi: 10.1109/TIP.2003.819861.